Thermodynamic properties of liquid water from a polarizable intermolecular potential

Tesfaye M. Yigzawe and Richard J. Sadus[a)]
Centre for Molecular Simulation, Swinburne University of Technology, PO Box 218, Hawthorn, Victoria 3122, Australia

(Received 20 November 2012; accepted 4 January 2013; published online 25 January 2013)

Molecular dynamics simulation results are reported for the pressure, isothermal pressure coefficient, thermal expansion coefficient, isothermal and adiabatic compressibilities, isobaric and isochoric heat capacities, Joule-Thomson coefficient and speed of sound of liquid water using a polarizable potential [Li *et al.*, J. Chem. Phys. **127**, 154509 (2007)]. These properties were obtained for a wide range of temperatures and pressures at a common liquid density using the treatment of Lustig [J. Chem. Phys. **100**, 3048 (1994)] and Meier and Kabelac [J. Chem. Phys. **124**, 064104 (2006)], whereby thermodynamic state variables are expressible in terms of phase-space functions determined directly from molecular dynamics simulations. Comparison with experimental data indicates that the polarizable potential can be used to predict most thermodynamic properties with a very good degree of accuracy.
 [http://dx.doi.org/10.1063/1.4779295]

I. INTRODUCTION

It is difficult to overstate the importance of water because it has a role in many biological, chemical, physical, and technical processes. Therefore, considerable emphasis has been placed on modelling and predicting the properties of water, some of which have well-documented anomalies.[1] Early attempts to predict the properties of water involved either empirical correlations or equation of state modelling.[2,3] From a practical perspective such approaches have considerable merit but they only provide a limited theoretical insight into the underlying nature of intermolecular interactions, which ultimately determine water's properties. In contrast, when used properly, molecular simulation[4] provides unambiguous information regarding the merit of the underlying model. Furthermore, molecular simulation can be increasingly used to provide worthwhile predictions to both guide and supplement experimental work.

Except for "on-the-fly" methods,[5] the use of molecular simulation requires the *a priori* postulation of an intermolecular potential to evaluate inter-particle forces or energies. As reviewed elsewhere[6] there are many alternative intermolecular potentials for water, which reflects the difficulty of accurately predicting its diverse properties. The most widely used models are rigid and variants of either the four-site[7] transferable interaction potential (TIP4P) or the three-site simple point charge (SPC, SPC/E) models.[8,9] The basis of many of these potentials is at best semi-empirical, although some recent progress[10] has been made in developing intermolecular potentials from first principles.

An aspect that is missing from many intermolecular potentials is the contribution of polarization, which is increasingly being recognized[11–15] as an important contribution to the properties of water. Polarizable potentials approximate the effect of multibody interactions that arise because the induced dipole of each molecule generates an electric field that affects all other molecules. For example, the Gaussian core polarizable model[11] yields a considerable improvement for the simultaneous prediction of various properties, including the diffusion coefficient. Recently, considerable success has been reported[16,17] using the Matsuoka-Clementi-Yoshimine non-additive[18] (MCYna) potential, which combines an *ab initio* two-body potential with an explicit evaluation of induction forces.

The prediction of thermodynamic properties is of fundamental importance in many processes and as such it is an important test for the intermolecular potential. Despite this, molecular simulation of the thermodynamic properties for water, and indeed other molecular systems, reported in the literature[19–33] is often confined to quantities such as pressure (p), energy (E), isochoric (C_v), and isothermal (C_p) heat capacities. In contrast, other thermodynamic properties such as the isothermal pressure coefficient (γ_v), thermal expansion coefficient (α_p), isothermal (β_T), and adiabatic (β_S) compressibilities, Joule-Thomson coefficient (μ_{JT}), and the speed of sound (w_0) are much less commonly reported. This absence of data is illustrated in Table I, which compares predictions of various intermolecular potentials. For the intermolecular potentials summarized in Table I, we could not find values in the literature for γ_v, β_S, or μ_{JT}. It is apparent from Table I that there are considerable differences in the values of both C_v and C_p predicted by the various intermolecular potentials. There is reasonable agreement with experiment for β_T between the different potentials whereas, in most instances, α_p is very inaccurately predicted.

The incomplete comparison in Table I can be partly attributed to the fact that only a few thermodynamic properties can be observed directly from conventional molecular simulations. For example, temperature (T), potential energy (U), and pressure (p) are the only directly observable quantities from microcanonical (NVE) ensemble simulations with a constant number of particles (N), volume (V), and energy (E). This

a)E-mail: rsadus@swin.edu.au.

TABLE I. Comparison with experiment for the thermodynamic properties predicted by various intermolecular potentials for liquid water at 298 K and 0.1 MPa.

Potential	C_v (J/mol K)	C_p (J/mol K)	β_T (1/GPa)	ω_0 (m/s)	α_p (10^{-4}/K)	Ref.
SPC		84.516	0.461		7.51	19
SPC/E		77.613	0.446		5.14	20
TIP3P		70.291	0.495		8.56	19
SPC/Fw		114.516	0.45		4.98	21
SPC/Fd		116.148	0.454		5.08	21, 22
TIP4P		80.751	0.67		9.4	23
TIP4P/2005		79.077	0.463			19
MCY	62.341			3040		24, 29
MCYL	73.638			3130		25
MCYna	74.357	74.63	0.448	1498.4	2.63	This work
ST2	87.864	92.885	0.63		− 6.9	26
TIP5P		122	0.46		6.7	23
NveD		101	0.56		2.8	27
IAPWS-95	74.836	75.770	0.448	1505.1	2.54	28
Experiment	74.44	75.338	0.458	1496.7	2.57	30–33

means that the calculation of other thermodynamic quantities requires the use of fluctuation formulas or equations of state. In contrast, Lustig[34–37] showed that, in principle, it is possible to calculate all thermodynamic state variables from key derivatives obtained directly from either molecular dynamics (MD) or Monte Carlo simulations. The method is based on the exact expressions for the thermodynamic state variables reported by Pearson *et al.*[38] using a Laplace transform technique for the microcanonical ensemble. Cağin and Ray[39,40] used this technique to derive expressions in the $NVE\vec{P}$ and $NVT\vec{P}$ ensembles, which also maintain a constant linear momentum ($\vec{P}$). Lustig[34–37] extended the method to systems of rigid polyatomic molecules. Meier and Kabelac[41] developed further improvements of this technique, which involves an additional quantity ($\vec{G}$) that is related to the initial position of the center of mass. This means that MD simulations are conducted in an $NVE\vec{P}\vec{G}$ ensemble. The approach has also been recently extended to the canonical ensemble.[42]

The advantage of the $NVE\vec{P}\vec{G}$ method is that it allows us to directly obtain all the thermodynamic quantities of a fluid from a MD simulation. Previous work has indicated[16–18] that polarization effects, as described by the MCYna potential, have a significant influence on such properties as the dielectric constant and structure of water. The aim of this work is to use the $NVE\vec{P}\vec{G}$ method to evaluate the ability of the MCYna potential to predict the thermodynamic properties of liquid water.

II. MD SIMULATIONS

A. Overview of the $NVE\vec{P}\vec{G}$ method

The method has been discussed in detail elsewhere[34,39,41–43] and only a brief outline of the salient features is given here. The fundamental equation of state for the system is defined by the entropy (S) postulate, i.e.,[41]

$$S(N, V, E, \vec{P}, \vec{G}) = k \ln \mathbf{\Omega}(N, V, E, \vec{P}, \vec{G}), \tag{1}$$

where $\mathbf{\Omega}(N, V, E, \vec{P}, \vec{G})$ is the phase-space volume and k is the Boltzmann constant. The basic phase-space functions are then introduced as an abbreviation representing the derivatives of the phase-space volume with respect to the independent thermodynamic state variables:

$$\Omega_{mn} = \frac{1}{\omega} \frac{\partial^{m+n} \Omega}{\partial E^m \partial V^n}, \tag{2}$$

where ω is the phase-space density. The exact derivation of the phase-space function is quite involved[41] resulting in a general expression given by

$$\begin{aligned}\Omega_{m\,n} = &\left(\frac{N}{V}\right)^n \frac{1}{N^n} (-1)^m \frac{2}{F-3} \left(-\frac{F-3}{2}\right)_m (-1)^n \left(-[N-1]\right)_n \left\langle K^{-(m-1)} \right\rangle \\ &+ (1-\delta_{0n}) \sum_{i=1}^{n} \binom{n}{i} (-1)^{n-i} \left(-[N-1]\right)_{n-i} \left(\frac{N}{V}\right)^{n-i} \frac{1}{N^{n-i}} \\ &\times \frac{2}{F-3} \sum_{l=1}^{i} (-1)^{m+l} \left(-\frac{F-3}{2}\right)_{m+l} \left\langle K^{-(m+l-1)} \left(\sum_{k=1}^{kmax(i,l)} c_{ilk} W_{ilk} \right) \right\rangle, \end{aligned} \tag{3}$$

TABLE II. Relations of thermodynamic state variables in terms of phase-space functions.

Temperature	$T = \left(\frac{\partial E}{\partial S}\right)_V = \frac{\Omega_{00}}{k}$
Pressure	$p = T\left(\frac{\partial S}{\partial V}\right)_E = \Omega_{01}$
Isochoric heat capacity	$C_V = \left[\left(\frac{\partial^2 S}{\partial E^2}\right)_V\right]^{-1} = k\left(1 - \Omega_{00}\Omega_{20}\right)^{-1}$
Isothermal pressure coefficient	$\gamma_V = \left(\frac{\partial p}{\partial T}\right)_V = k\frac{\Omega_{11} - \Omega_{01}\Omega_{20}}{1 - \Omega_{00}\Omega_{20}}$
Isothermal compressibility	$\beta_T^{-1} = -V\left(\frac{\partial p}{\partial V}\right)_T = V\left[\frac{\Omega_{01}(2\Omega_{11} - \Omega_{01}\Omega_{20}) - \Omega_{00}\Omega_{11}^2}{1 - \Omega_{00}\Omega_{20}} - \Omega_{02}\right]$
Adiabatic compressibility	$\beta_S^{-1} = -V\left(\frac{\partial p}{\partial V}\right)_S = V\left[\Omega_{01}\left(2\Omega_{11} - \Omega_{01}\Omega_{20}\right) - \Omega_{02}\right]$
Speed of sound	$w_0^2 = -\frac{V^2}{M}\left(\frac{\partial p}{\partial V}\right)_S = \frac{V^2}{M}\left[\Omega_{01}\left(2\Omega_{11} - \Omega_{01}\Omega_{20}\right) - \Omega_{02}\right]$
Thermal expansion coefficient	$\alpha_P = \beta_T\,\gamma_V$
Isobaric heat capacity	$C_P = C_V\frac{\beta_T}{\beta_S}$
Joule-Thomson coefficient	$\mu_{JT} = V\frac{T\gamma_V\beta_T - 1}{C_P}$

which involves the sum of the degrees of freedom of all the molecules (F), ensemble averages of products of powers of the kinetic energy $K = E - U\left(\vec{r}^N\right)$, and volume derivatives of the potential energy $\partial^n U/\partial V^n$. In Eq. (3) and hereafter N is the number of water molecules and $\langle ... \rangle$ denotes ensemble averages. The $(x)_n = x(x+1)(x+2)\cdots(x+n-1)$ terms represent the Pochhammer symbol with $(x)_0 = 1$, where x is any quantity contained in the brackets, and δ_{ij} is the Kronecker delta. The term $c_{ilk}\,W_{ilk}$ is a product of certain volume derivatives of the potential energy $W_{ilk} = (-\partial^i U/\partial V^i)(-\partial^k U/\partial V^k)...$ and of multinomial coefficients c_{ilk} described in detail elsewhere.[41] The volume derivatives of nth order for the potential energy are given by

$$\frac{\partial^n U}{\partial V^n} = \frac{1}{3^n V^n}\sum_{i=1}^{N-1}\sum_{j=i+1}^{N}\sum_{k=1}^{n} a_{nk} r_{ij}^k \frac{\partial^k u}{\partial r_{ij}^k}, \tag{4}$$

where u is the intermolecular potential energy and r_{ij} denotes the distance between particle i and j. The coefficients a_{nk} are constructed using a recursion relation.[41] All thermodynamic state variables are then expressible in terms of the phase-space function. The resulting thermodynamic state variables used in this work are summarized in Table II and explicit expressions for the phase-space functions are given in the Appendix. From a practical perspective, simulations in the $NVE\vec{P}\vec{G}$ simply involve implementing a conventional $NVE\vec{P}$ simulation while keeping track of the volume derivatives of the intermolecular potential required for the evaluation of the thermodynamic quantities.

B. MCYna potential and simulation details

The $NVE\vec{P}\vec{G}$ MD simulations were performed for a homogenous fluid of water molecules interacting via the MCYna potential.[18] The MCYna potential is a polarizable extension of the *ab initio* Matsuoka-Clementi-Yoshimine (MCY) potential.[29] The MCYna potential treats the water molecule as a rigid triatomic system with two negative charges placed on hydrogen atoms and one positive charge placed on the bisector of the H–O–H angle near the oxygen atom. The MCYna intermolecular potential $u(r)$ for water is the sum of two-body additive u_2, non-additive three-body u_3, and polarizable u^{pol} contributions

$$u(\vec{r}) = \sum_{i<j}^{N} u_2(\vec{r}_i, \vec{r}_j) + \sum_{i<j<k}^{N} u_3(\vec{r}_i, \vec{r}_j, \vec{r}_j) + u^{pol}. \tag{5}$$

The contribution of two-body interactions was obtained from the *ab initio* MCY potential[29]

$$\begin{aligned} u_2 = {} & q^2\cdot\left(\frac{1}{r_{13}} + \frac{1}{r_{14}} + \frac{1}{r_{23}} + \frac{1}{r_{24}}\right) + \frac{4q^2}{r_{78}} \\ & - 2q^2\left(\frac{1}{r_{18}} + \frac{1}{r_{28}} + \frac{1}{r_{37}} + \frac{1}{r_{47}}\right) + a_1 e^{(-b_1 r_{56})} \\ & + a_2\left(e^{(-b_2 r_{13})} + e^{(-b_2 r_{14})} + e^{(-b_2 r_{23})} + e^{(-b_2 r_{24})}\right) \\ & + a_3\left(e^{(-b_3 r_{16})} + e^{(-b_3 r_{26})} + e^{(-b_3 r_{35})} + e^{(-b_3 r_{45})}\right) \\ & - a_4\left(e^{(-b_4 r_{16})} + e^{(-b_4 r_{26})} + e^{(-b_4 r_{35})} + e^{(-b_4 r_{45})}\right). \end{aligned} \tag{6}$$

The meaning of the parameters is the same as given in the literature[29] and their values are summarized in Table III. The benefit of an *ab initio* potential is that it should avoid many of the theoretical uncertainties of empirical intermolecular potentials, such as the need to fit the parameters of the potential to experimental data for various properties. However, in the absence of non-additive contributions, it has been demonstrated[18,24,29] that the original MCY potential[29] yields inaccurate results for the energy, dielectric constant, dipole moment, radial distribution functions, heat capacities, and speed of sound of water.

Non-additive contributions to intermolecular interactions arise for induction interactions, resulting from molecular polarizability, short-range repulsion, and dispersion interactions. It is well documented[18,44] that multibody dispersion interactions can be adequately described using the Axilrod-Teller[45] triple dipole term,

$$u_3 = \frac{\nu(1 + 3\cos\theta_i\cos\theta_j\cos\theta_k)}{(r_{ij}r_{ik}r_{jk})^3}, \tag{7}$$

TABLE III. Intermolecular parameters used in MCYna intermolecular potentials. Unless otherwise stated, all values are in atomic units.

Parameter	Value
a_1	1734.1960
a_2	1.061887
a_3	2.319395
a_4	0.436006
b_1	2.726696
b_2	1.460975
b_3	1.567367
b_4	1.181792
q^2	0.514783
r_{OH}	0.957200
r_{OM}	0.505783
θ_{HOH} (deg)	104.52
α (Å^3)	1.44
β (dimensionless)	0.557503
ν	287.944

where θ_i, θ_j, and θ_k are inside angles of the triangle formed by three atoms denoted by i, j, and k, and r_{ij}, r_{ik}, and r_{jk} are the three side lengths of the triangle. The parameter ν is the non-additive coefficient, which can be determined from experiment.[46] The theoretical background and rationale for using this formula is given elsewhere.[18] The contribution of multibody non-additive polarization interactions was obtained from[41]

$$u^{pol} = -\frac{1}{2}\sum_{i=1}^{N} \vec{\mu}_i^{ind} \cdot \vec{E}_i^{o}, \tag{8}$$

where $\vec{E}_i^{o}$ is the electrostatic field of surrounding charges and $\vec{\mu}_i^{ind}$ is the induced dipole at site i given by

$$\vec{\mu}_i^{ind} = \alpha\beta \cdot \vec{E}_i = \alpha\beta \cdot \left[\vec{E}_i^{o} + \sum_{j=1, j\neq i}^{N} T_{ij}\vec{\mu}_j^{ind}\right]. \tag{9}$$

In Eq. (8) $\alpha\beta$ is the polarizability and T_{ij} is the dipole tensor:

$$T_{ij} = \frac{1}{4\pi\varepsilon_o r_{ij}^5}\left[3r_{ij}r'_{ij} - r_{ij}^2\right]. \tag{10}$$

The main computational cost for the MCYna potential is the evaluation of the three-body terms via Eq. (7). Although we have performed these calculations here, past experience[18] indicates that induction interactions represent the most important non-additive contribution. Calculating induction interactions via Eq. (9) typically[18,47] doubles the computation time compared with simple intermolecular potentials such as the SPC/E potential. Further details of the calculation procedure are also available elsewhere.[16–18,47]

Other polarizable potentials are available in the literature,[11–15] although their usefulness for thermodynamic properties has not been tested extensively. A feature of some polarizable water potentials is that they incorporate either Lennard-Jones[48] or exponential-6 interactions,[49] which means that the non-additive contribution to intermolecular interactions is not clearly identified. The advantages of the MCYna potential are that it has a two-body term that is based on an *ab initio* calculation and an explicit non-additive contribution.

The simulations were performed at a constant density of 55.371 dm^3/mol (i.e., 0.998 g/cm^3 or 100 molecules per nm^3). At this density water is in the liquid phase for a wide range of temperatures enabling calculations between 298 K and 645 K. The system consisted of 500 water molecules confined to a cubic box and subject to periodic boundary conditions. The simulations were conducted for 500 000 time steps with a time interval of 2 *f*s with the first 400 000 steps used for equilibration.

There are electrostatic, three body and polarization interactions in the MCYna model. The induced dipole moment was calculated using the conjugate gradient method.[18] An Ewald summation was used for Columbic interactions with a convergence parameter of $\alpha = 5.0/L$. The real-space cutoff for the Ewald sum was L/2 where L is the box length, the reciprocal-space cutoff was 5/2L, and the screening parameter was set to 5.6/L. A spherical cutoff radius equal to half the box length, 12.331 Å was used to evaluate the forces and energies. The SHAKE algorithm[4,50] with the Verlet leapfrog integrator[4] was used to constrain the molecular structure.

For the MCYna potential there is one polarizable site on the negative charge center of each water molecule. For simplicity, intramolecular interactions are ignored, which means that the induced dipole does not interact with the partial charge on the same water molecule. The gas phase polarizability coefficient[1] of 1.44 Å^3 results in a value for the dipole moment in the liquid phase, which does not agree with experiment. To improve the accuracy, a scaling factor[18] of $\beta = 0.557503$ was used, which results in a polarizability coefficient of 0.802804 Å^3. This gives a dipole moment of 2.9 D, with 0.9 D attributed to induction interactions. Three-body interaction is assumed only between oxygen atoms because of the electron poor feature of hydrogen. In the absence of an experimental value, the value of the non-additive coefficient of oxygen was assumed to be 5/9 the value for argon, which reflects the relative size difference of the two atoms.

III. RESULTS AND DISCUSSION

A. Reference data for water

Ideally, simulation results should be compared directly with experimental data. However, almost all experimental results for water reported in the literature are at isobaric conditions whereas the MD simulations in the $NVE\vec{P}\vec{G}$ ensemble yield isochoric values. Therefore, we must either convert the data or find an accurate alternative to the experimental values. For this purpose, we have used the International Association for the Properties of Water and Steam (IAPWS-95) software developed by Wagner[28] to calculate thermodynamic quantities at isochoric conditions. IAPWS-95 is based on a highly accurate empirical equation of state[3] for water. The accuracy of such calculations are apparent from the comparison given in Table I in which the IAPWS-95 results are in very close agreement with experimental values for C_V, C_p, β_T, α_p, and w_0. The comparison indicates that IAPWS-95 may

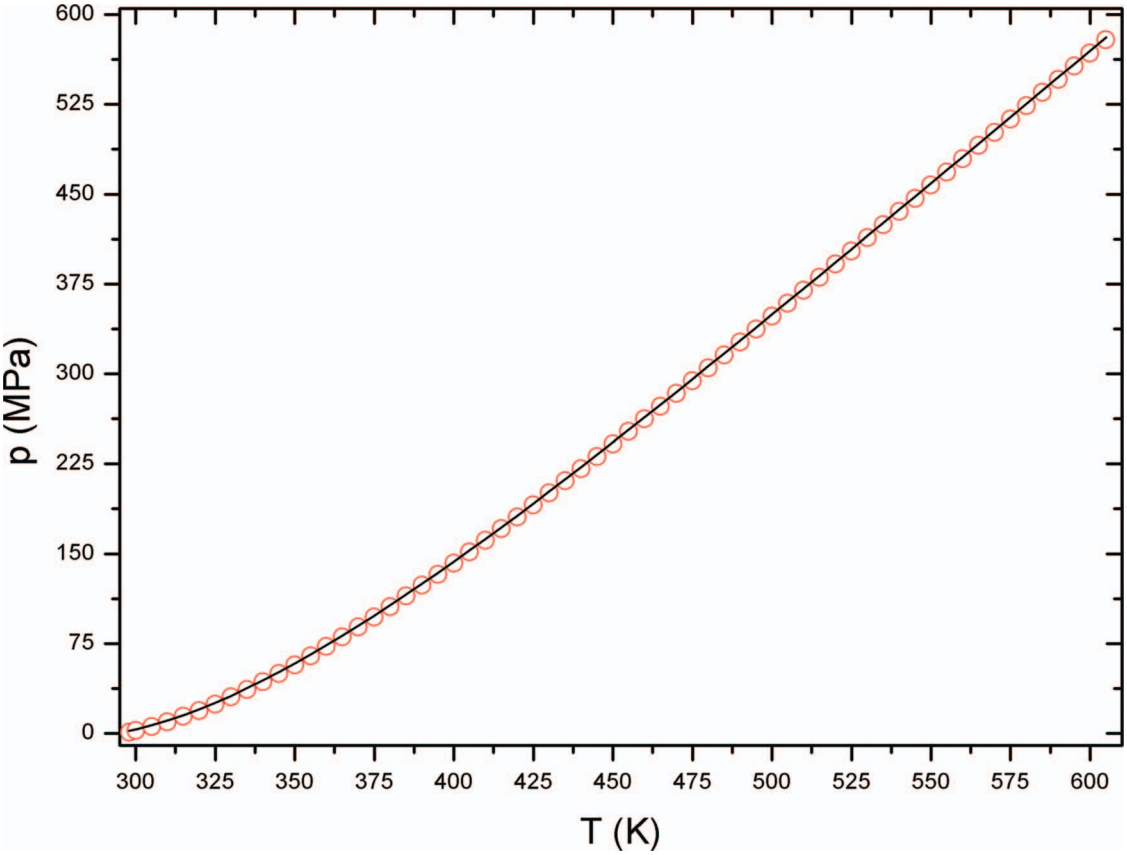

FIG. 1. Pressure as a function of temperature predicted by the MCYna potential (red ○) and compared to reference data[28] for water (——). Error bars for this and subsequent figures are not illustrated because the statistical uncertainties in the simulations are typically smaller than the size of the symbols.

yield values that are slightly higher than experimental values but the difference is probably within experimental uncertainty. IAPWS-95 can only be used to directly calculate p, C_V, C_p, μ_{JT}, and w_0. The remaining thermodynamic quantities, namely β_T, β_S, γ_v, and α_p are calculated from the IAPWS-95 outputs using the following well-known relationships:[51]

$$\left.\begin{aligned} \beta_s &= \frac{V}{w_0^2 M} \\ \beta_T &= \frac{\beta_s C_p}{C_V} \\ \gamma_V^2 &= \frac{C_V\left(\beta_s^{-1} - \beta_T^{-1}\right)}{T\,V} \\ \alpha_p &= \frac{\mu_{JT} C_p}{TV} + \frac{1}{T} \end{aligned}\right\}, \tag{11}$$

where M is the total mass of the system. It should be noted that the MCYna results are pure predictions and absolutely no attempt has been made to optimize agreement with experiment.

B. Pressure

The pressure of liquid water as a function of temperature from our simulations is compared with accurate reference data[28] in Fig. 1. The pressure of water is an almost linearly increasing function of temperature. The pressure calculated from our simulation is in very good agreement with the reference data over the entire range of temperatures. The pressure from simulations at a temperature less than 290 K (not shown in Fig. 1) is negative, which implies that water is in a metastable state. Negative pressures for metastable water have been reported previously.[52,53]

C. Isothermal and adiabatic compressibilities

The isothermal compressibility is positive in the one phase region. For an ordinary liquid isothermal compressibility increases with temperature as it becomes less dense. In contrast, at constant pressure, experimental values[52,54] of the isothermal compressibility of water pass through a temperature minimum before increasing with temperature like an ordinary fluid.[55] A comparison with experiment at 0.1 MPa over the temperature range of 260 K to 360 K for the TIP5P, TIP4P, TIP4P/2005, and SPC/E potentials has been reported by Pi *et al.*[56] There are large deviations from experiment for the TIP5P, TIP4P, and SPC/E potentials, particularly at higher temperatures. In contrast, the TIP4P/2005 potential yields good agreement.

Simulation results for the isothermal compressibility of water as a function of temperature are compared with reference data in Fig. 2. Unlike the constant pressure data, our results at constant volume correspond to a range of pressures as is illustrated in Fig. 1. This means that the values of β_T from both simulation and the reference data[28] continue to decrease with increasing temperature. At low temperatures, the

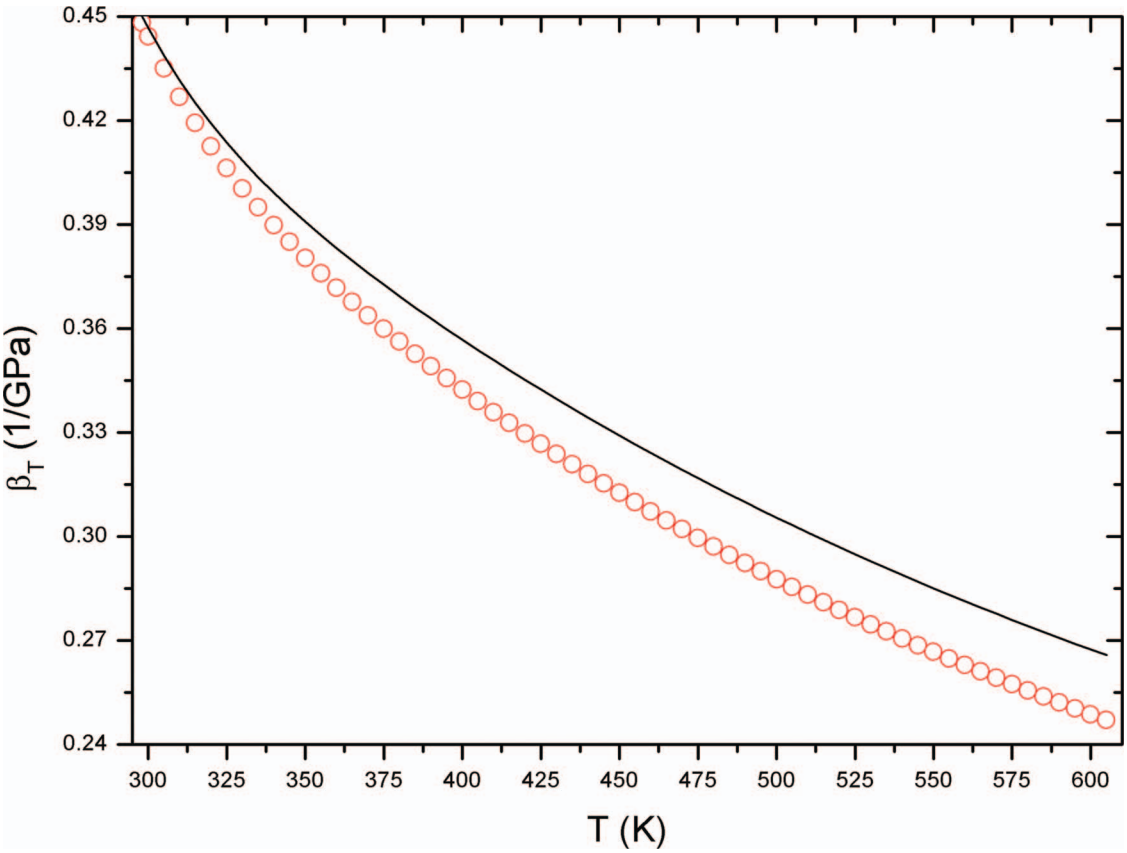

FIG. 2. Isothermal compressibility as a function of temperature predicted by the MCYna potential (red ○) and compared to reference data[28] for water (——).

isothermal compressibility predicted by the MCYna potential is in very good agreement with the reference data obtained from IAPWS-95. However, as the temperature is increased the simulation results increasingly under predict the reference data. The quality of agreement with the reference data is similar to the results obtained[57] for the TIP4P/2005 potential.

Results for the adiabatic compressibility of water are compared with reference data in Fig. 3. The adiabatic compressibilities obtained from the MCYna potential are in very good agreement with the reference data at all temperatures. In particular, the agreement for temperatures below 400 K is exceptionally good, whereas at higher temperatures a relatively small degree of under prediction becomes increasingly apparent. This provides an interesting contrast with the results for the isothermal compressibilities (Fig. 2), which display much larger deviations from the reference data.

D. Isothermal pressure coefficient

Simulation results for the isothermal pressure coefficient are compared with reference data for water in Fig. 4. In the temperature range of 298 K to 425 K, the isothermal pressure coefficients obtained using the MCYna water potential are in very close agreement with the results from IAPWS-95. At higher temperatures, the simulation results under predict the isothermal coefficient but the agreement is nonetheless reasonably good. Experimentally, the isothermal pressure coefficient becomes negative in the phase-space region with anomalous density behavior.[43] The observation that the isothermal pressure coefficient is positive for the entire simulation region implies that water does not show anomalies at a density of 0.998 g/cm^3.

E. Thermal expansion coefficient

The thermal expansion coefficient is the measure of the tendency of matter to change volume in response to a change in temperature. The thermal expansion coefficient as a function of temperature is illustrated in Fig. 5. Experimentally, the thermal expansion coefficient increases almost linearly until it reaches its peak value at 430 K and then it decreases. This means the tendency of water to change volume is most apparent when the temperature is between 400 K and 450 K. It is apparent from the comparison given in Fig. 5 that the MCYna water potential closely mimics the behavior of the reference data. At all temperatures, the MCYna potential only slightly under predicts the true value of the thermal expansion coefficient. The MCYna potential predicts a maximum value of 6.629×10^{-4} K^{-1} at 445 K. These good results contrast with the failure of other intermolecular potentials (Table I). For example, at 298 K the value of α_p predicted by the SPC/E and TIP4P potentials, exceed the experimental value by approximately 200% and 365%, respectively.

F. Isochoric and isothermal heat capacities

The isochoric heat capacity of water as a function of temperature from our simulation and reference data[28] is

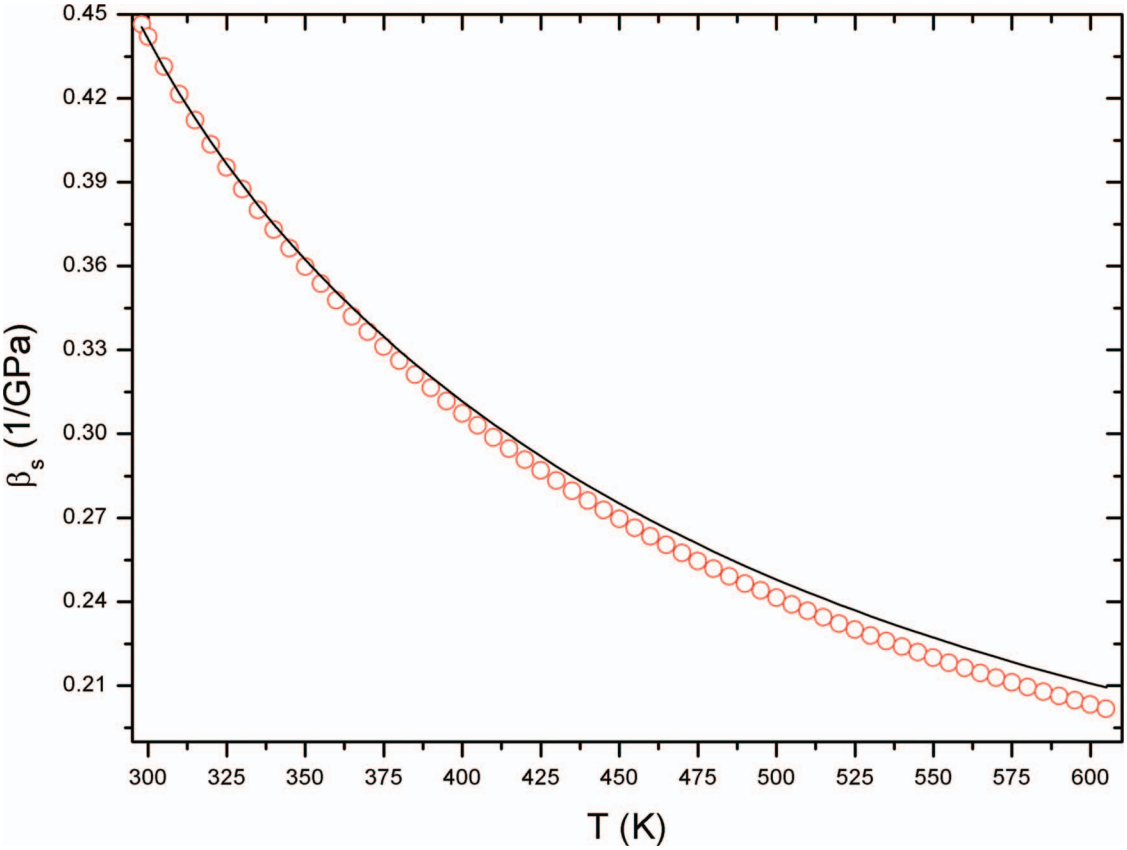

FIG. 3. Adiabatic compressibility as a function of temperature predicted by the MCYna potential (red ○) and compared to reference data[28] for water (——).

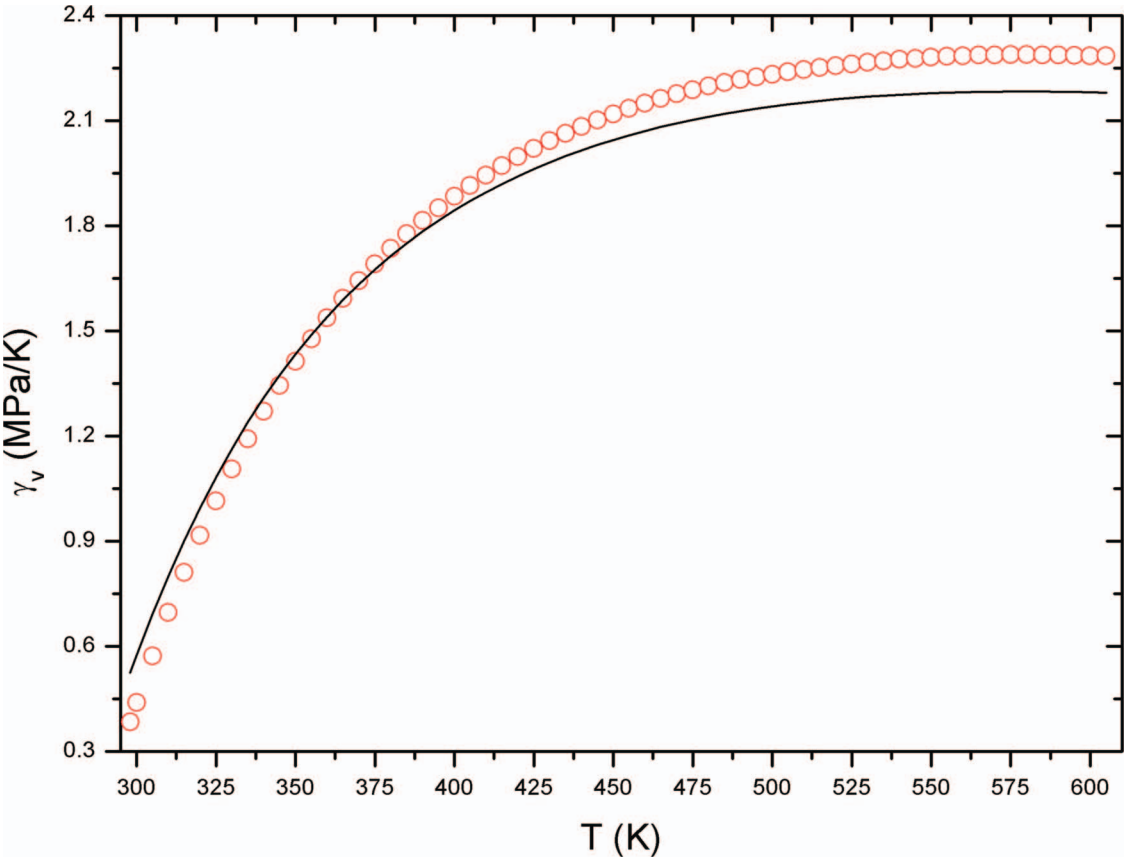

FIG. 4. Isothermal pressure coefficient as a function of temperature predicted by the MCYna potential (red ○) and compared to reference data[28] for water (——).

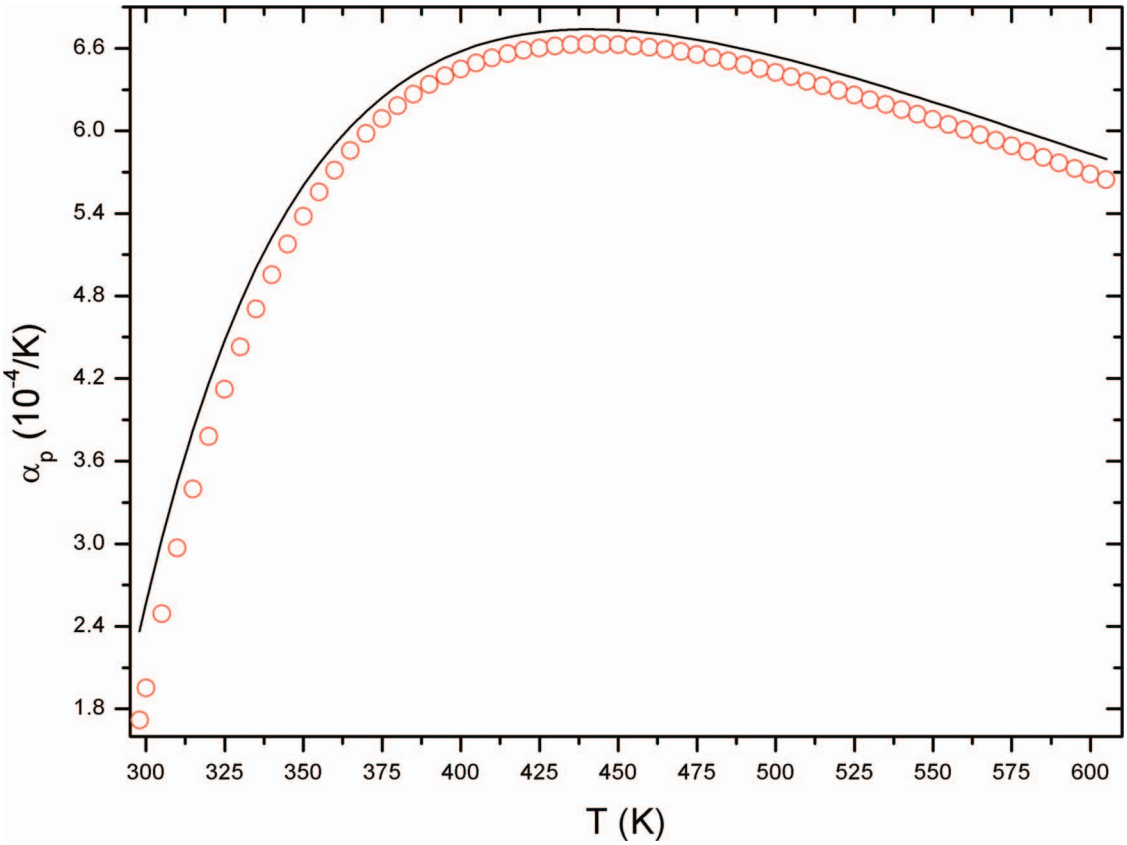

FIG. 5. Thermal expansion coefficient as a function of temperature predicted by the MCYna potential (red ○) and compared to reference data[28] for water (——).

illustrated in Fig. 6. The isochoric heat capacity decreases progressively with increasing temperature. The comparison with reference data in Fig. 6 shows that the MCYna potential can be used to accurately calculate the isochoric heat capacity for the entire range of temperatures (298 K to 645 K) at which water is a liquid. The average percentage deviation between the simulation and reference data over the entire temperature range is 2.78%. We are unaware of a similar comparison for other intermolecular potentials. However, path integral molecular dynamics (PIMD) calculations of isochoric heat capacity of water vapor at temperatures up to 3000 K have been reported.[57] In contrast to our results for the liquid phase, quantum corrections were required[57] to obtain acceptable agreement with experimental results for water vapor. The PIMD calculations used a flexible variant of the SPC potential, which does not explicitly account for polarization.

The isobaric heat capacity of water as a function of temperature is compared with reference data in Fig. 7. The values of the isobaric heat capacity obtained from the MCYna potential under predicts the reference data at all temperatures, which is in sharp contrast to the very good agreement obtained for isochoric values (Fig. 6). As is evident from the relationships in Table II, the isobaric heat capacity is derived from the values of isochoric heat capacity and compressibilities. Therefore, an error in either of these thermodynamic quantities will be reflected in the results for the isobaric heat capacity. It is evident from Figs. 2, 3, and 6 that the MCYna potential under predicts all of these quantities, which at least partly accounts for the isobaric heat capacity results. It is apparent from the comparison of the isobaric heat capacities (Table I) calculated from other potentials that the MCYna potential nonetheless yields the best agreement with experiment. At 298 K and 0.1 MPa, the deviation from experiment is less than 1% compared with considerably larger discrepancies for the other potentials. It is of interest to note, that with the exception of TIP3P, all the potentials in Table I over predict the isobaric heat capacity whereas the MCYna potential under predicts it. Figure 7 indicates that this under prediction widens with increasing temperature. It is sometimes suggested[57] that the over prediction of heat capacity is caused by a failure to address quantum influences whereas the MCYna results also clearly demonstrate the importance of polarization as a key contributing factor.

Extensive data for other potentials at different temperatures are not available in the literature. A recent comparison with experiment for C_p calculated for the SPC/E potential reported by Bandyopadhyay *et al.*[58] indicates over prediction at low temperatures (260 K to 300 K) and under prediction at higher temperatures (320 K to 350 K). In contrast at pressures of both 0.1 MPa and 100 MPa, good agreement with experiment has been reported[57] for the TIP4P/2005 potential at temperatures between 240 K and 300 K.

G. Joule-Thomson coefficient

The Joule-Thomson effect describes the temperature change of a gas or liquid when it is forced through a valve or

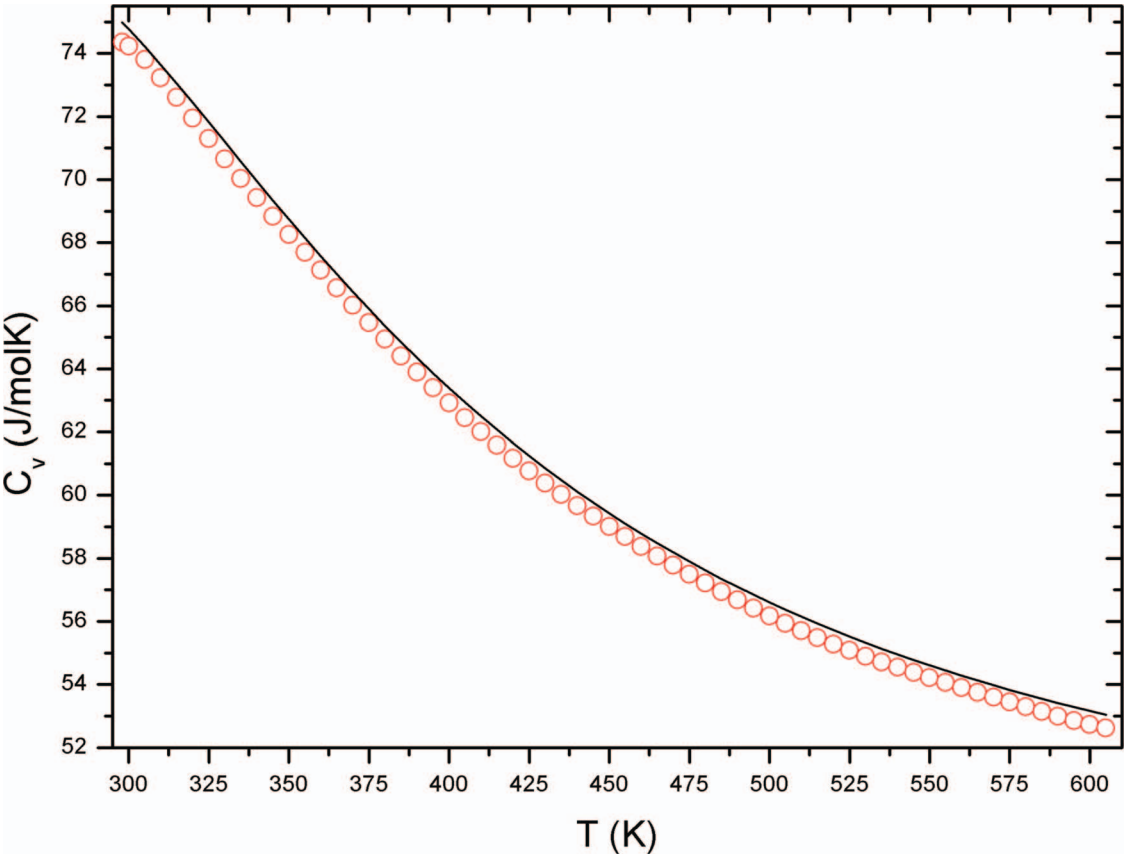

FIG. 6. Isochoric heat capacity as a function of temperature predicted by the MCYna potential (red ○) and compared to reference data[28] for water (——).

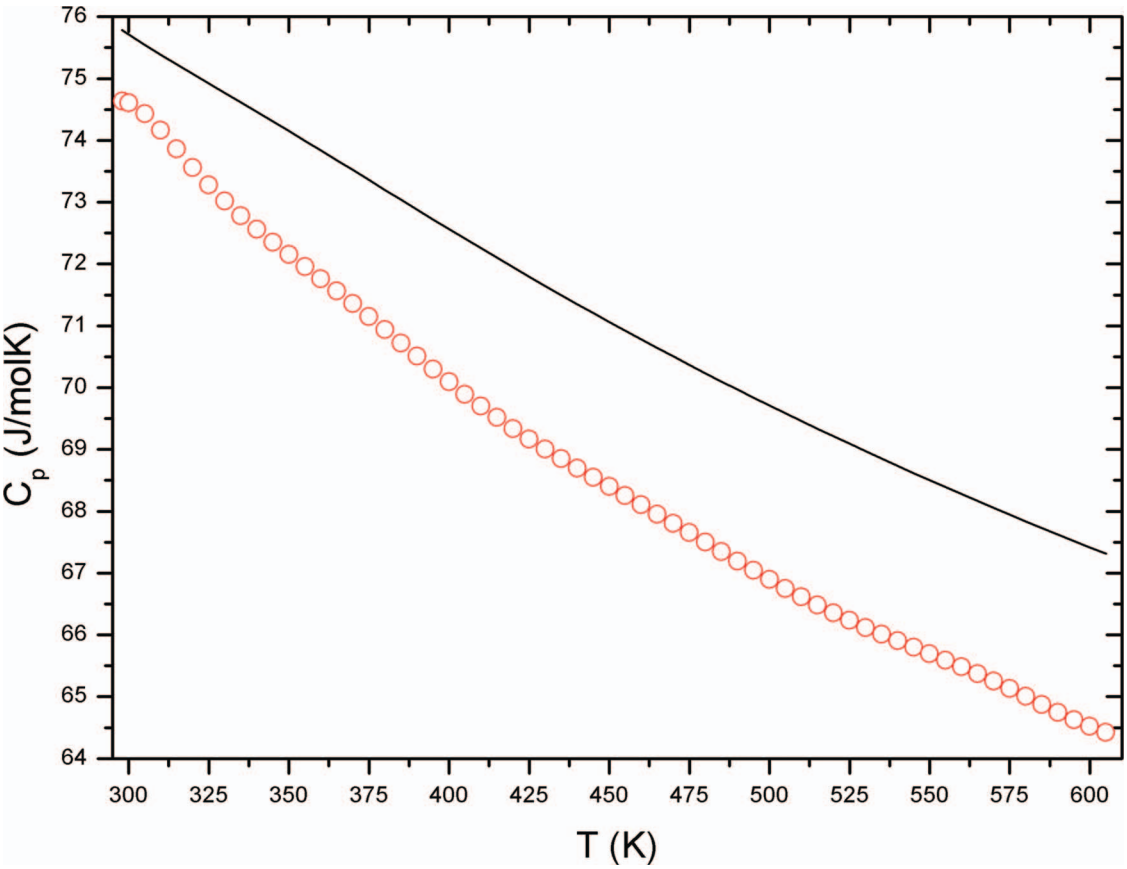

FIG. 7. Isobaric heat capacity as a function of temperature predicted by the MCYna potential (red ○) and compared to reference data[28] for water (——).

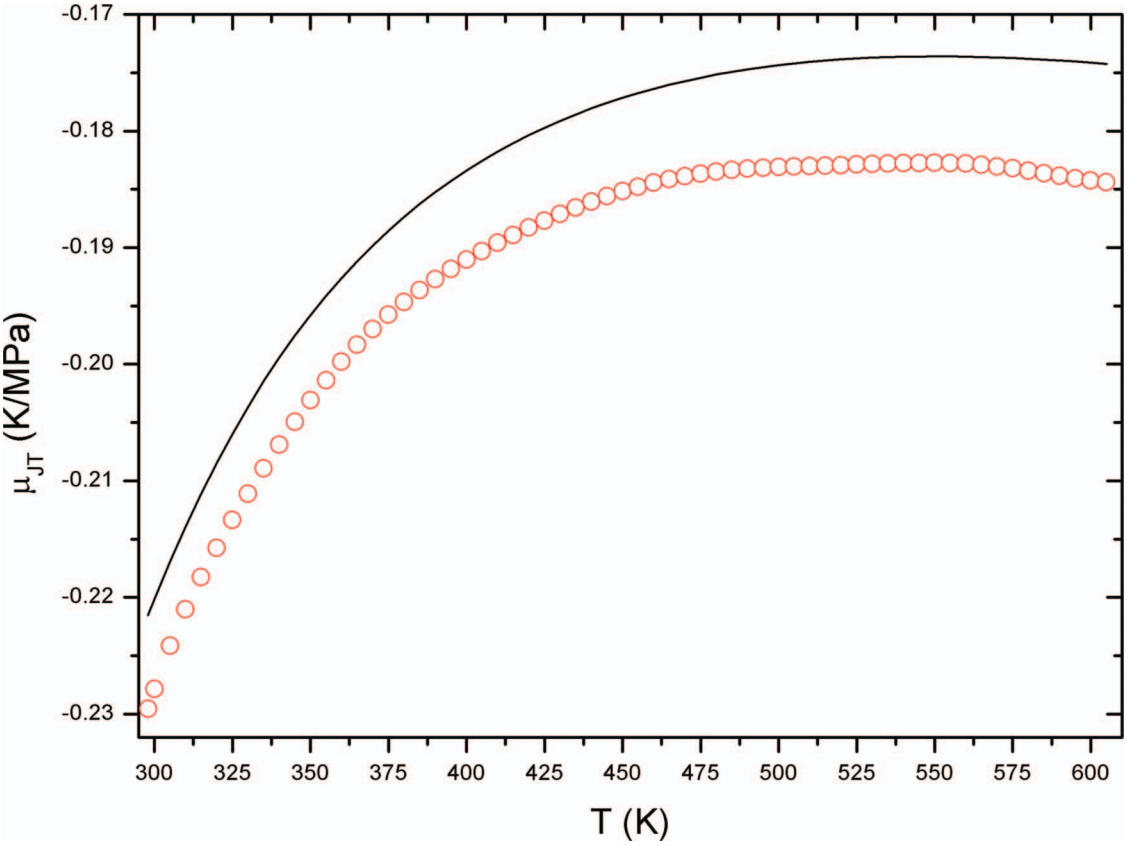

FIG. 8. Joule-Thomson coefficient as a function of temperature predicted by the MCYna potential (red ○) and compared to reference data[28] for water (——).

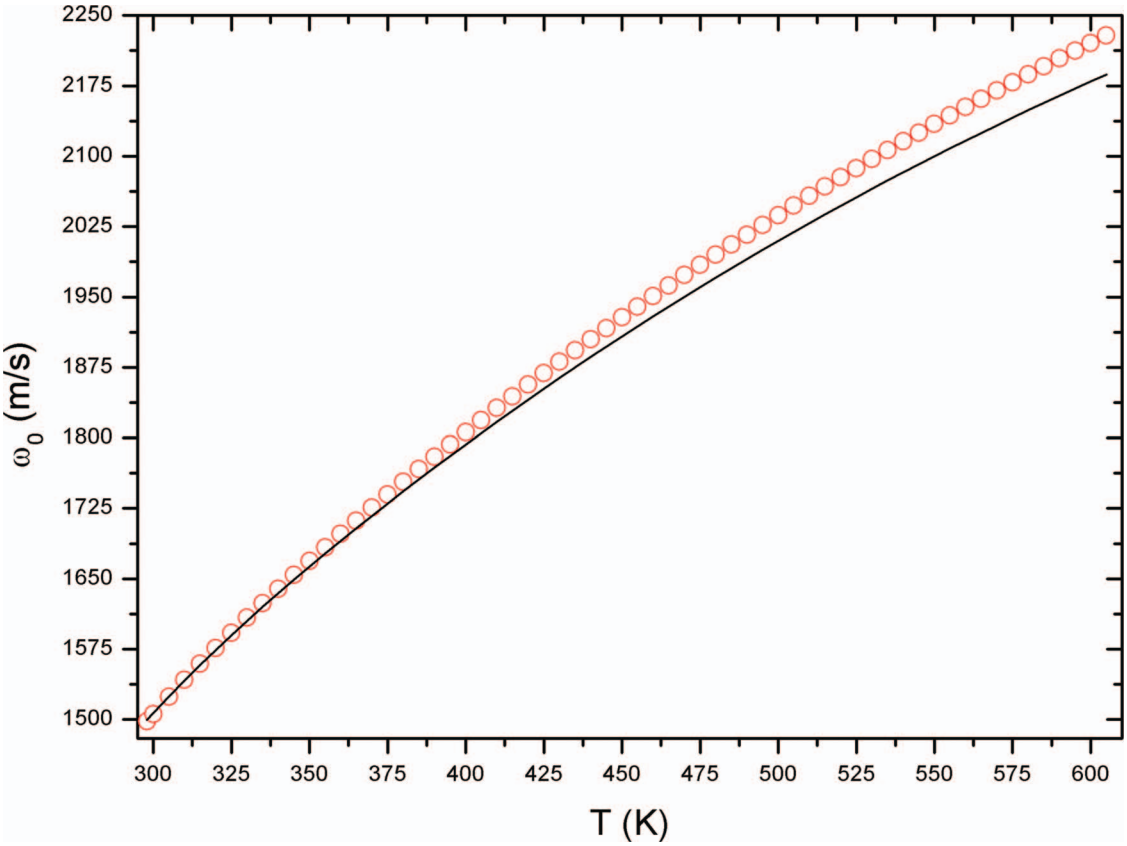

FIG. 9. Speed of sound as a function of temperature predicted by the MCYna potential (red ○) and compared to reference data[28] for water (——).

porous plug while kept insulated so that no heat is exchanged with the environment. The simulation results are compared with reference data in Fig. 8. The Joule-Thomson coefficient is negative for the entire simulation region, which indicates that there is no inversion curve (locus of $\mu_{JT} = 0$) for water at higher densities. The MCYna potential qualitatively reproduces the behavior of the reference data at all temperatures, although the value of the Joule-Thomson coefficient is under predicted. The disparity increases with increasing temperature. This is consistent with the trend observed for the isobaric heat capacity (Fig. 6). The simulated values of the Joule-Thomson coefficient are derived (Table II) from results obtained from the isobaric heat capacity, isothermal compressibility, and isothermal pressure coefficient and as such incorporates the uncertainties from all of these quantities, each of which under predict the reference data. There are no results for other commonly used intermolecular potentials to compare with the MCYna results.

H. Speed of sound

The speed of sound in water as a function of temperature is illustrated in Fig. 9. It is apparent from Fig. 9 that the MCYna potential yields good agreement with the reference data for temperatures between 298 K and 400 K. For T > 400 K the MCYna potential increasingly over predicts the speed of sound. The error increases with increasing temperature but arguably the maximum discrepancy of 2.19% at 645 K is acceptable. It is difficult to assess these very good results relative to other intermolecular potentials because, as the comparison in Table I indicates, there is no comparable data for other models. It is interesting to note that the original MCY potential, which forms the underlying basis of the MCYna potential, greatly over predicts the speed of sound compared with experimental data. The main difference between the MCYna and MCY potentials is the inclusion of polarization effects in the former, which suggest that this is an important factor in the observed improvement in agreement with experiment.

IV. CONCLUSIONS

The $NVE\vec{P}\vec{G}$ MD ensemble can be used to directly obtain all of the thermodynamic properties of water. Results obtained for the pressure, adiabatic compressibility, isothermal pressure coefficient, thermal expansion coefficient, isochoric heat capacity, and speed of sound using the MCYna potential are in very good agreement with reference data over the entire liquid range of temperatures. In some cases, the agreement is almost exact indicating that polarization has a major influence. The isothermal compressibilities, isobaric heat capacities, and Joule-Thomson coefficients are under predicted. In part, the discrepancy in the isobaric heat capacity can be attributed to the uncertainty in the calculated isothermal compressibility. The fact that the calculation of the Joule-Thomson coefficient requires knowledge of both the isobaric heat capacity and the isothermal compressibility probably accounts for the uncertainty in this quantity. Nonetheless the results for these properties reproduce the experimentally observed trends. The comparison with results obtained for other intermolecular potentials is unavoidably incomplete because of the absence of data for other models. However, for the limited cases for which data are available, it is clear that incorporating polarization in the MCYna potential has resulted in a considerable improvement in the accuracy of predictions for the thermodynamic properties of water.

The MCYna calculations included three-body interactions, which are computationally expensive. However, the contribution of induction interactions dominates and, for practical applications, the three-body calculations can be omitted without a material loss of accuracy. In the absence of three-body interactions, the MCYna potential is computationally competitive with other intermolecular potentials for water.

ACKNOWLEDGMENTS

We thank the National Computing Infrastructure (NCI) for an allocation of computing time. One of us (T.M.Y.) thanks Swinburne University of Technology for a postgraduate research award.

APPENDIX: EVALUATION OF PHASE-SPACE FUNCTIONS

Equations (A1)–(A6) are the explicit expressions for the phase-space functions reported elsewhere[41] when $\vec{P} = 0$. They are used to evaluate the thermodynamic quantities in Table II,

$$\mathbf{\Omega}_{00} = kT = \frac{2}{F-3}\langle K\rangle, \tag{A1}$$

$$\mathbf{\Omega}_{10} = 1, \tag{A2}$$

$$\mathbf{\Omega}_{01} = \frac{N-1}{V}kT - \left\langle \frac{\partial U}{\partial V}\right\rangle, \tag{A3}$$

$$\mathbf{\Omega}_{11} = \frac{N-1}{V} + \left[1 - \frac{F-3}{2}\right]\left\langle K^{-1}\left(\frac{\partial U}{\partial V}\right)\right\rangle, \tag{A4}$$

$$\mathbf{\Omega}_{20} = -\left[1 - \frac{F-3}{2}\right]\left\langle K^{-1}\right\rangle, \tag{A5}$$

$$\mathbf{\Omega}_{02} = \frac{2(N-2)(N-1)}{(F-3)V^2}\langle K\rangle - \left[1-\frac{F-3}{2}\right]\left\langle K^{-1}\left(\frac{\partial U}{\partial V}\right)^2\right\rangle - \left\langle \frac{\partial^2 U}{\partial V^2}\right\rangle - \frac{2(N-1)}{V}\left\langle \frac{\partial U}{\partial V}\right\rangle. \tag{A6}$$

[1] D. Eisenberg and W. Kauzmann, *The Structure and Properties of Water* (Clarendon, Oxford, 2005); E. Brunner, M. C. Thies, and G. M. Schneider, J. Supercrit. Fluids **39**, 160 (2006); V. M. Shmonov, R. J. Sadus, and E. U. Franck, J. Phys. Chem. **97**, 9054 (1993).

[2] Y. S. Wei and R. J. Sadus, AIChE J. **46**, 169 (2000); A. E. Mather, R. J. Sadus, and E. U. Franck, J. Chem. Thermodyn. **25**, 771 (1993);

N. G. Sretenskaja, R. J. Sadus, and E. U. Franck, J. Phys. Chem. **99**, 4273 (1995).
[3]W. Wagner and A. Pruß, J. Phys. Chem. Ref. Data **31**, 387 (2002).
[4]R. J. Sadus, *Molecular Simulation of Fluids: Theory, Algorithms and Object-Orientation* (Elsevier, Amsterdam, 1999); R. J. Sadus, Mol. Phys. **87**, 979 (1996).
[5]R. Car and M. Parrinello, Phys. Rev. Lett. **55**, 2471 (1985).
[6]C. Vega, J. L. F. Abascal, M. M. Conde, and J. L. Aragones, Faraday Discuss. **141**, 251 (2009); B. Guillot, J. Mol. Liq. **101**, 219 (2002).
[7]W. L. Jorgensen, J. Chandrasekhar, J. D. Madura, R. W. Impey, and M. L. Klein, J. Chem. Phys. **79**, 926 (1983).
[8]H. J. C. Berendsen, J. P. M. Postma, W. F. van Gunsteren, and J. Hermans, in *Intermolecular Forces*, edited by B. Pullman (Reidel, Dordrecht, 1981).
[9]H. J. C. Berendsen, J. R. Grigera, and T. P. Straatsma, J. Phys. Chem. **91**, 6269 (1987).
[10]R. Bukowski, K. Szalewicz, G. C. Groenboom, and A. van der Avoird, Science **315**, 1249 (2007).
[11]P. Paricaud, M. Prědota, A. A. Chialvo, and P. T. Cummings, J. Chem. Phys. **122**, 244511 (2005).
[12]G. Lamoureux, E. Harder, I. V. Vorobyov, B. Roux, and A. D. MacKerell, Jr., Chem. Phys. Lett. **418**, 245 (2006).
[13]G. Delgado-Barrio, R. Prosmiti, P. Villarreal, G. Winter, J. S. Medina, B. González, J. V. Gomez, P. S. Sangrá, J. J. Santana, and M. E. Torres, in *Frontiers in Quantum Systems in Chemistry and Physics*, edited by S. Wilson, P. J. Grout, G. Delgado-Barrio, J. Maruani, and P. Piecuch (Springer, Berlin, 2008), Vol. 18, p. 351.
[14]G. Raabe and R. J. Sadus, J. Chem. Phys. **134**, 234501 (2011).
[15]G. Raabe and R. J. Sadus, J. Chem. Phys. **137**, 104512 (2012).
[16]I. Shvab and R. J. Sadus, Phys. Rev. E **85**, 051509 (2012).
[17]I. Shvab and R. J. Sadus, J. Chem. Phys. **137**, 124501 (2012).
[18]J. Li, Z. Zhou, and R. J. Sadus, J. Chem. Phys. **127**, 154509 (2007).
[19]C. Vega and J. L. F. Abascal, J. Chem. Phys. **123**, 144504 (2005).
[20]L. A. Báez and P. Clancy, J. Chem. Phys. **101**, 9837 (1994).
[21]Y. Wu, H. L. Tepper, and G. A. Voth, J. Chem. Phys. **124**, 024503 (2006).
[22]L. X. Dang and B. M. Pettitt, J. Phys. Chem. **91**, 3349 (1987).
[23]M. W. Mahoney and W. L. Jorgensen, J. Chem. Phys. **112**, 8910 (2000).
[24]R. W. Impey, P. A. Madden, and I. R. McDonald, Mol. Phys. **46**, 513 (1982).
[25]G. C. Lie and E. Clementi, Phys. Rev. A **33**, 2679 (1986).
[26]F. H. Stillinger and A. Rahman, J. Chem. Phys. **60**, 1545 (1974).
[27]H. Nada and J. J. M. van der Eerden, J. Chem. Phys. **118**, 7401 (2003).
[28]W. Wagner, See http://www.thermo.rub.de/en/prof-w-wagner/software/iapws-95.html. The IAPWS-95 software used to obtain reference data for water is available from this website.
[29]O. Matsuoka, E. Clementi, and M. Yoshimine, J. Chem. Phys. **64**, 1351 (1976).
[30]A. K. Soper and M. G. Phillips, Chem. Phys. **107**, 47 (1986).
[31]L. Haar, J. S. Gallagher, and G. S. Kell, *NBS/NRC Steam Tables* (Hemisphere, Washington, DC, 1984).
[32]S. Kell, J. Chem. Eng. Data **20**, 97 (1975).
[33]N. E. Dorsey, *Properties of Ordinary Water-Substance in All Its Phases: Water-Vapor, Water, and All the Ices* (Reinhold, New York, 1940).
[34]R. Lustig, J. Chem. Phys. **100**, 3048 (1994).
[35]R. Lustig, J. Chem. Phys. **100**, 3060 (1994).
[36]R. Lustig, J. Chem. Phys. **100**, 3068 (1994).
[37]R. Lustig, J. Chem. Phys. **109**, 8816 (1998).
[38]E. M. Pearson, T. Halicioglu, and W. A. Tiller, Phys. Rev. A **32**, 3030 (1985).
[39]T. Cağin and J. R. Ray, Phys. Rev. A **37**, 247 (1988).
[40]T. Cağin and J. R. Ray, Phys. Rev. A **37**, 4510 (1988).
[41]K. Meier and S. Kabelac, J. Chem. Phys. **124**, 064104 (2006).
[42]R. Lustig, Mol. Simul. **37**, 457 (2011); Mol. Phys. **110**, 3041 (2012).
[43]P. Mausbach and R. J. Sadus, J. Chem. Phys **134**, 114515 (2011).
[44]G. Marcelli and R. J. Sadus, J. Chem. Phys. **111**, 1533 (1999).
[45]B. M. Axilrod and E. Teller, J. Chem. Phys. **11**, 299 (1943).
[46]P. J. Leonard and J. A. Barker, in *Theoretical Chemistry: Advances and Perspectives*, edited by H. Eyring and D. Henderson (Academic, London, 1975), Vol. 1.
[47]J. Li, Z. Zhou, and R. J. Sadus, Comput. Phys. Commun. **178**, 384 (2008).
[48]J. Caldwell, L. X. Dang, and P. A. Kollman, J. Am. Chem. Soc. **112**, 9144 (1990).
[49]A. Wallqvist, P. Ahlström, and G. Karlström, J. Chem. Phys. **94**, 1649 (1990).
[50]J. P. Ryckaert, G. Ciccotti, and H. J. C. Berendsen, J. Comput. Phys. **23**, 327 (1977).
[51]A. Münster, *Classical Thermodynamics*, translated by E. S. Halberstadt (Wiley, London, 1970).
[52]P. H. Poole, F. Sciortino, U. Essmann, and H. E. Stanley, Nature (London) **360**, 324 (1992).
[53]H. E Stanley, M. C. Barbosa, S. Mossa, P. A Netz, F. Sciortino, F. W. Starr, and M. Yamada, Physica A **315**, 281 (2002).
[54]P. G. Debenedetti, J. Phys: Condens. Matter **15**, R1669 (2003).
[55]J. L. Finney, Philos. Trans. R. Soc. London, Ser. B **359**, 1145 (2004).
[56]H. L. Pi, J. L. Aragones, C. Vega, E. G. Noya, J. L. F. Abascal, M. A. Gonzalez, and C. McBride, Mol. Phys. **107**, 365 (2009).
[57]W. Shinoda and M. Shiga, Phys. Rev. E **71**, 041204 (2005); M. Shiga and W. Shinoda, J. Chem. Phys. **123**, 134502 (2005).
[58]D. Bandyopadhyay, S. Mohan, S. K. Ghosh, and N. Choudhury, J. Chem. Eng. Data **57**, 1751 (2012).